

Research Paper

Radiative MHD Walter's Liquid-B Flow Past a Semi-Infinite Vertical Plate in the Presence of Viscous Dissipation with a Heat Source

Chenna Kesavaiah DAMALA¹⁾, Venkateswarlu BHUMARAPU^{2)*},
Oluwole Daniel MAKINDE³⁾

¹⁾ *Department of Basic Sciences & Humanities
Vignan Institute of Technology and Science*

Deshmukhi (V), Yadadri-Bhuvanagiri (Dist), T.S, India
e-mail: chennakesavaiah@gmail.com

²⁾ *Department of Mathematics, Walchand Institute of Technology
Solapur, M.H, India*

*Corresponding Author e-mail: bvenkateswarlu.maths@gmail.com

³⁾ *Faculty of Military Science, Stellenbosch University
South Africa
e-mail: makinded@gmail.com*

The free convective magnetohydrodynamics (MHD) flow of a non-Newtonian fluid due to a semi-infinite vertical plate under the influence of radiation and viscous dissipation is investigated. The system of partial differential equations is derived and solved for the solutions of velocity and temperature profiles along with the Nusselt number and skin friction by using the perturbation technique. The related important dimensionless parameters of Eckert, Grashof, and Prandtl numbers, magnetic field, radiation and heat source are discussed and shown in graphs. Also, the Nusselt number and skin friction at the plate are obtained and presented in the tabular forms. Finally, the corresponding result of Newtonian fluid is obtained by setting viscoelastic parameter $k_1 = 0$. It is worth mentioning that the obtained results coincide with the previously published results.

Key words: radiation; magnetohydrodynamics (MHD); viscous dissipation; porous medium; heat source and viscoelastic fluid; vertical plate.

NOTATIONS

$B(x)$ – applied magnetic field,

B_0 – constant,

C – concentration of the fluid,

C_f – skin friction coefficient,

- C_m – solid surface concentration,
 C_p – specific heat at constant pressure,
 c_s – heat capacity of the fluid,
 C_∞ – concentration far away from the plate,
 Ec – Eckert number,
 $f(\eta)$ – dimensionless stream function,
 Gr – Grashof number,
 H – dimensionless melting parameter,
 k^* – mean absorption coefficient,
 k – thermal conductivity,
 Kr – chemical reaction parameter,
 M – magnetic field parameter,
 Nu – Nusselt number,
 Pr – Prandtl number,
 Q – heat source parameter,
 q_r – radiative heat flux,
 R – thermal radiation parameter,
 Re_x – Reynolds number,
 Sh – Sherwood number,
 T – temperature of the fluid,
 T'_w – temperature of the fluid at the plate,
 T_S – solid surface temperature,
 T_∞ – temperature far away from the plate,
 U_w – constant velocity,
 U_∞ – free stream velocity,
 (uv) – velocity components,
 (xy) – Cartesian coordinates.

Greek symbols

- ε – moving parameter,
 ν – kinematic viscosity,
 α – thermal conductivity of the fluid,
 ρ – density of the fluid,
 σ – electrical conductivity of the fluid,
 σ^* – Stefan-Boltzmann constant,
 η – similarity variable,
 λ – latent heat of the fluid,
 μ – coefficient of viscosity,
 τ_w – wall shear stress,
 ψ – stream function,
 $\theta(\eta)$ – dimensionless temperature.

Subscripts

- w – condition at the wall,
 ∞ – condition at the free stream.

1. INTRODUCTION

The problem of free convective flow under the influence of the magnetic field has attracted the interest of many researchers because of its application in different engineering fields, including geophysics, environmental and technical problems, in designing ventilating and heating of buildings, cooling of electronic components in nuclear reactors, post-accident heat removal from pebble-bed nuclear reactors, bed thermal storage, pollutant dispersion in aquifers, solar power collector, and heat sink in the turbine blades. In addition, convective flows driven by temperature differences of the bounding walls of channels are important in industrial applications.

Variable suction of two-dimensional free convective flow past an infinite plate due to viscous dissipation and heat sources was studied by POP and SOUNDALGEKAR [1]. SINGH and COWLING [2] analyzed the effect of magnetic field on the free convective flow of electrically conducting fluids past a semi-infinite plate. SACHETI *et al.* [3] used the Laplace transform technique for the solutions of free convective flow over a moving vertical plate with magnetic field and heat flux. SATTAR and ALAM [4] investigated the effects of a Hall current on the magnetohydrodynamics (MHD) convective flow over a porous vertical plate by using the Runge-Kutta-Merson integration method. SAHOO *et al.* [5] analyzed the effects of suction/injection on the free convective flow over a porous vertical plate with a magnetic field. The influence of the MHD convective flow of Jeffery fluid due to ramped wall effects on velocity and temperature was examined by MAQBOOL *et al.* [6]. HAMZA [7] carried out the finite difference process for the convective flow of an exothermic fluid in a vertical channel. The free convective flow of nanofluid through a vertical plate was presented by NISA *et al.* [8] and HAJZADEH *et al.* [9]. SHAH *et al.* [10], GHOLINIA *et al.* [11], WANG and ZHOU [12], and PATEL [13] studied the free convective flow mechanism.

The influence of thermal radiation and heat transfer convective flow is observed in several manufacturing sectors, in the design of high precision equipment as well as industrial and environmental applications. The applications are found mostly in nuclear power plants, gas turbines, cooling chambers, fossil fuel combustion, energy processes, astrophysical flows, propulsion devices for aircraft, and solar power technology. Moreover, thermal radiation effects on the free convection flow are important in the context of space technology and many engineering applications, such as in advanced types of power plants for nuclear rockets, re-entry vehicles, high-speed flights, and procedures involving high temperatures.

The Rosseland diffusion approximation is valid for optically thick media. The radiative heat fluxes approximated for an optically dense medium by the Rosseland diffusion approximation have been used extensively in many studies related

to radiation. CHAMKHA [14] inspected a finite difference scheme for the boundary layer flow caused by a semi-infinite vertical surface with radiation and heat source/sink. Heat transfer of nanofluid flow past a porous vertical plate along with a rotating system in the presence of heat source and radiation was implemented by SATYA NARAYANA *et al.* [15]. Their study intended to enhance nanofluid particles with heat transfer. CORTELL [16] implemented the second-grade and Walter's liquid-B fluids models on radiative nonlinear heat transfer of a viscoelastic flow due to a stretching sheet with a magnetic field. AMIR HAMZAH *et al.* [17] examined the radiation energy on squeezed magnetohydrodynamics (MHD) flow of nanofluids between two infinite parallel plates. They concluded that there was no significant difference between the Runge-Kutta-Fehlberg scheme with the shoot technique and the optimal homotopy asymptotic method. FAGBADE *et al.* [18] studied the radiation effects on the convective flow of viscoelastic fluid over a stretching surface with a magnetic field. They solved the resultant equation using the spectral homotopy analysis method. The research presented in [19, 20] studied radiation and heat source/sink in various physical geometries of the flow.

Deformation and flow of materials require energy. This mechanical energy is dissipated, i.e., during the flow, it is converted into the internal energy of the material. Viscous dissipation is of interest in many applications. For example, significant temperature rises were observed in polymer processing flows such as injection moulding or extrusion at high rates. Aerodynamic heating in the thin boundary layer around high-speed aircraft increases the temperature of the skin. In a completely different application, the dissipation function is used to define the viscosity of the dilute suspension. The influence of viscous dissipation is a significant factor in the heat transfer process, especially for highly viscous flows, even with moderate velocities. The energy equation is added by viscous dissipation, which transforms the kinetic energy to internal energy due to viscosity and hence increases the fluid motion. Therefore, the fluid motion is controlled by a dimensionless parameter called the Eckert number.

MAKANDA *et al.* [21] studied the convective viscoelastic fluid caused by a porous cone with viscous dissipation. They obtained the solutions by the successive linearization method and found that the temperature changes linearly along the cone's surface. The viscous dissipation effect on non-Newtonian Casson fluid flow due to stretching sheet with variable thermal conductivity was examined by VENKATESWARLU and SATYA NARAYANA [22]. They observed that the heat and mass transfer rates are controlled by thermal conductivity. HAYAT *et al.* [23] presented the variable viscosity of non-Newtonian Casson fluid flow through the stretching cylinder with viscous dissipation by using the homotopic analysis. Radiation and viscous dissipation of nanofluid flow with the magnetic field was inspected by NAYAK [24]. KHAN *et al.* [25],

HAYAT *et al.* [26], RAMESH [27] and MUHAMMAD *et al.* [28] examined the viscous dissipation and Joule heating of non-Newtonian fluid flows induced by a magnetic field. VENKATESWARLU *et al.* [29] evaluated the melting and viscous dissipation effects on boundary layer flow over a moving surface with magnetic field.

Viscoelastic fluid flow phenomena play an important role in various manufacturing and engineering applications such as liquid crystals, carbon fibers, crude oil, food and rheological processing. Viscous dissipation for a fluid with suspended particles is equated to the viscous dissipation of a pure Newtonian fluid, both being the same flow (same macroscopic velocity gradient). EZZAT and ABD-ELAAL [30] examined the viscoelastic boundary layer flow due to a porous vertical surface. Their intention was to study the effects of cooling and heating on viscoelastic fluids. The MHD viscoelastic fluid flow over a stretching sheet with variable viscosity was researched by PRASAD *et al.* [31]. The authors derived the equations using the Runge-Kutta integration scheme together with a shooting method and found that the skin friction decreased with a superior magnetic field. GOYAL and BHARGAVA [32] presented the numerical solution of viscoelastic nanofluid flow due to a stretching sheet caused by slip and heat source. The convective heat transfer of viscoelastic fluid flow due to a porous permeable wedge with radiation and magnetic field was presented by RASHIDI *et al.* [33]. The authors found that the wedge angle enhances with heat transfer to the fluid. VENKATESWARLU and SATYA NARAYANA [34] analyzed the viscoelastic fluid flow over a porous vertical surface with a magnetic field. They derived the solutions by the regular perturbation method. The heat transfer of viscoelastic fluid flow caused by a vertical stretching sheet with the magnetic field was summarized by LI *et al.* [35]. They concluded that the characteristics of viscoelastic flow and heat transfer are predicted by relaxation time. BILAL *et al.* [36] implemented the two-dimensional viscoelastic fluids due to a stretching surface with the magnetic field. The authors used $\Lambda = 0$ and reduced the formulation of the problem to classical Fourier's problem. The stagnation point flow of nanofluid due to a convectively heated stretching surface with the magnetic field was studied by SATYA NARAYANA *et al.* [37]. DESSIE and KISHAN [39] studied the variable viscosity and viscous dissipation effects on MHD flow over a stretching sheet. BESTHAPU *et al.* [40] studied the convection flow of MHD nanofluid over an exponentially stretching surface due to viscous dissipation by using the finite difference scheme.

Motivated by the works mentioned above, this work aims to investigate a Walter's liquid-B fluid model for free convective flow due to a porous vertical plate with constant suction and a heat source. The velocity and temperature are presented graphically for various values of the parameters. Further, the skin friction and the Nusselt number are studied via graphs and tables.

The Walters's liquid-B fluid model of constitutive equation is

$$(1.1) \quad \sigma^{ik} = \sigma_{ik} - pg_{ik} \quad \text{and} \quad \sigma_{ik} = 2\eta_0 e^{ik} - 2k_0 e^{ik},$$

where p is the isotropic pressure, V_i is the velocity vector, σ^{ik} is the stress tensor, and g_{ik} is the metric tensor of a fixed coordinate system X^i .

The contravariant form of e^{ik} is given by

$$(1.2) \quad e^{ik} = v^m e_m^{ik} - v^k e_m^{im} - v^i e_m^{mk} + \frac{\partial e^{ik}}{\partial t}.$$

The converted derivative of the deformation rate tensor e^{ik} is defined by

$$(1.3) \quad 2e^{ik} = v_{i,k} + v_{k,i}.$$

The limiting viscosity η_0 at the small rate of shear is given by

$$(1.4) \quad \eta = \int_0^\infty N(\tau) d\tau \quad \text{and} \quad k_0 = \int_0^\infty \tau N(\tau) d\tau,$$

where $N(\tau)$ is the relaxation spectrum. This idealized model is a valid approximation of Walters's liquid-B model B taking very short memories into account so that terms involving

$$(1.5) \quad \int_0^\infty t^n N(\tau) d\tau, \quad n \geq 2$$

are neglected.

2. MATHEMATICAL FORMULATION

Consider a two-dimensional unsteady MHD flow of a viscoelastic fluid past a semi-infinite tilted porous plate. Let α be the angle and which is made by the vertical plate. The x -axis is taken along the plate and the y -axis is considered normal to the plate. A uniform magnetic field of strength B_0 is applied along the y -axis normal to the plate. Assume that, initially, the fluid and plate are at the same temperature in a stationary condition. At the time $t > 0$, the plate is given an impulsive motion in the direction of flow against gravity with the constant velocity U_0 and the plate temperature varies linearly with time.

The equations of the flow can be written as:

$$(2.1) \quad \frac{\partial v'}{\partial y'} = 0,$$

$$(2.2) \quad \frac{\partial u'}{\partial t'} + V' \frac{\partial u'}{\partial y'} = \nu \frac{\partial^2 u'}{\partial y'^2} - \frac{k_0}{\rho} \left\{ \frac{\partial^3 u'}{\partial y'^2 \partial t'} + V' \frac{\partial^3 u'}{\partial y'^3} \right\} + g\beta (T' - T'_\infty) - \frac{\sigma\beta_0^2}{\rho} u',$$

$$(2.3) \quad \frac{\partial T'}{\partial t'} + V' \frac{\partial T'}{\partial y'} = K \frac{\partial^2 T'}{\partial y'^2} - \frac{1}{\rho C_p} \frac{\partial q_r}{\partial y'} + \frac{\nu}{C_p} \left\{ \frac{\partial u'}{\partial y'} \right\}^2 - \left\{ \frac{1}{4} \frac{\partial u'}{\partial y'} \frac{\partial^3 u'}{\partial y' \partial t'} + V' \frac{\partial u'}{\partial y'} \frac{\partial^2 u'}{\partial y'^2} \right\} - \frac{Q_0}{\rho C_p} (T' - T'_\infty),$$

where ρ is the fluid density, ν is the kinematic viscosity, σ is a fluid electrical conductivity, β is the thermal coefficient of expansion, g is the acceleration due to gravity, k is thermal conductivity, T' is the temperature of the plate, T'_∞ is the free stream temperature, q_r is the radiative heat flux along the y -direction, k_0 is the viscoelastic parameter, C_p is the specific heat at constant pressure, x' , y' represent the distances along and perpendicular to the plate and t' is the time, and u' , v' are the velocity components along x' and y' , respectively.

The initial and boundary conditions are

$$(2.4) \quad \begin{aligned} u' = 0, \quad V' = -V_0, \quad T'_w = T'_w + \varepsilon(T'_w - T'_\infty)e^{i\omega t'} \quad \text{at } y' = 0, \\ u' \rightarrow \infty, \quad T' \rightarrow T'_\infty \quad \text{as } y' \rightarrow \infty, \end{aligned}$$

where V_0 is a constant of integration, and a negative sign indicates that the suction is towards the plate.

The radiative heat flux q_r under the Rosseland approximation, is

$$(2.5) \quad q_r = -\frac{4\sigma_1 \partial T'^4}{3k_1 \partial y'},$$

where k_1 is the mean absorption coefficient and σ_1 is the Stefan-Boltzmann constant.

Assume that the temperature difference within the flow is so small that T'^4 can be expressed as a linear function of T' . This is obtained by expanding T'^4 in a Taylor series about T'_∞ and neglecting the higher-order terms, so we obtain:

$$(2.6) \quad T'^4 \cong 4T'^3_\infty T' - 3T'^4_\infty.$$

Using Eqs (2.5) and (2.6) in Eq. (2.3), the equation of energy becomes

$$(2.7) \quad \frac{\partial T'}{\partial t'} + V' \frac{\partial T'}{\partial y'} = K \frac{\partial^2 T'}{\partial y'^2} + \frac{16\sigma_1 T'^3_\infty}{3k_1} \frac{\partial^2 T'}{\partial y'^2} + \frac{\nu}{C_p} \left(\frac{\partial u}{\partial y} \right)^2 - k_0 \left\{ \frac{1}{4} \frac{\partial u'}{\partial y'} \frac{\partial^3 u'}{\partial y' \partial t'} + V' \frac{\partial u'}{\partial y'} \frac{\partial^2 u'}{\partial y'^2} \right\} - \frac{Q_0}{\rho C_p} (T' - T'_\infty).$$

The suitable non-dimensional variables are defined as:

$$\begin{aligned}
 (2.8) \quad y &= \frac{y'V_0}{\nu}, & t &= \frac{t'V_0^2}{4\nu}, & \phi &= \frac{Q_0\nu}{\rho C_p V_0^2}, \\
 T &= \frac{T' - T'_\infty}{T'_w - T'_\infty}, & k_1 &= \frac{k_0 V_0^2}{\rho \nu^2}, & \text{Ec} &= \frac{V_0^2}{C_p (T'_w - T'_\infty)}, \\
 \text{Pr} &= \frac{\nu}{K}, & u &= \frac{u'}{V_0}, & K &= \frac{k_0}{\rho C_p}, \\
 N &= \frac{kk_1}{4\sigma 1T_\infty^3}, & M &= \frac{\sigma B_0^2 \nu}{\rho V_0^2}, & \text{Gr} &= \frac{g\beta\nu(T'_w - T'_\infty)}{V_0^2}.
 \end{aligned}$$

Using Eq. (2.8), we get the following non-dimensional equations:

$$(2.9) \quad \frac{1}{4} \frac{\partial u}{\partial t} - \frac{\partial u}{\partial y} = \frac{\partial^2 u}{\partial y^2} - k_1 \left\{ \frac{1}{4} \frac{\partial^3 u}{\partial y^2 \partial t} - \frac{\partial^3 u}{\partial y^3} \right\} + \text{Gr} T - Mu,$$

$$\begin{aligned}
 (2.10) \quad \frac{1}{4} \text{Pr} \frac{\partial T}{\partial t} - \text{Pr} \frac{\partial T}{\partial y} &= \beta_1 \frac{\partial^2 T}{\partial y^2} - \text{Pr} \text{Ec} \left\{ \frac{\partial u}{\partial y} \right\}^2 \\
 &\quad - k_1 \text{Pr} \left\{ \frac{1}{4} \frac{\partial u}{\partial y} \frac{\partial^2 u}{\partial y \partial t} - \frac{\partial u}{\partial y} \frac{\partial^2 u}{\partial y^2} \right\} - \frac{1}{4} \varphi \text{Pr} T,
 \end{aligned}$$

where $\beta_1 = \left(\frac{3N + \text{Pr}}{3N} \right)$, Ec is the Eckert number, Gr is the Grashof number, M is the magnetic number, Pr is the Prandtl number, φ is the heat source parameter, k_1 is the viscoelastic parameter, N is the radiation parameter, and K is the thermal conductivity.

The modified boundary conditions are

$$\begin{aligned}
 (2.11) \quad u &= 0; & T &= 1 + \varepsilon e^{i\omega t} & \text{at } y &= 0, \\
 u &\rightarrow 0; & T &\rightarrow 0 & \text{as } y &\rightarrow \infty.
 \end{aligned}$$

For solving Eqs (2.9) and (2.10), we can use the perturbation technique and the parameter $\varepsilon \ll 1$, the temperature and velocity field in the region are considered as:

$$\begin{aligned}
 (2.12) \quad u(y, t) &= \varepsilon e^{i\omega t} u_1(y) + u_0(y), \\
 T(y, t) &= \varepsilon e^{i\omega t} T_1(y) + T_0(y).
 \end{aligned}$$

On substituting Eqs (2.12) in Eqs (2.9) and (2.10) and equating the like powers of ε , we obtain:

$$(2.13) \quad k_1 u_0''' + u_0'' + u_0' - M u_0 = -\text{Gr } T_0,$$

$$(2.14) \quad k_1 \left\{ u_1''' - \frac{i\omega}{4} u_1'' \right\} + u_1'' + u_1' - \left\{ \frac{i\omega}{4} + M \right\} u_1 = \text{Gr } T_1,$$

$$(2.15) \quad \beta_1 T_0'' + \text{Pr } T_0' - \frac{1}{4} \text{Pr } \phi T_0 = -\text{Ec Pr } (u_0')^2 - k_1 \text{Pr } u_0' u_0'',$$

$$(2.16) \quad \beta_1 T_1'' + \text{Pr } T_1' - \frac{1}{4} \text{Pr } (\varphi - i\omega) T_1 = -2\text{Ec Pr } u_0' u_1' + k_1 \text{Pr } \left\{ \frac{i\omega}{4} u_0' u_1' - u_1' u_0'' - u_0' u_1'' \right\},$$

where the prime denotes the differentiation with respect to y .

The corresponding boundary conditions are

$$(2.17) \quad \begin{array}{llll} u_0 = 0, & u_1 = 0, & T_0 = 1, & T_1 = 1 \quad \text{at} \quad y = 0, \\ u_0 \rightarrow 0, & u_1 \rightarrow 0, & T_0 \rightarrow 0, & T_1 \rightarrow 0 \quad \text{as} \quad y \rightarrow \infty. \end{array}$$

In order to solve Eqs (2.13) to (2.16), we use the multi-parameter perturbation technique and assume $\text{Ec} \ll 1$, thus we write

$$(2.18) \quad \begin{array}{ll} u_0 = u_{00}(y) + \text{Ec } u_{01}(y), & T_0 = T_{00}(y) + \text{Ec } T_{01}(y), \\ u_1 = u_{10}(y) + \text{Ec } u_{11}(y), & T_1 = T_{10}(y) + \text{Ec } T_{11}(y). \end{array}$$

Using Eqs (2.18) in Eqs (2.13) to (2.16) and equating the coefficient of like powers of Ec we get the following sets of differential equations:

$$(2.19) \quad k_1 u_{00}''' + u_{00}'' + u_{00}' - M u_{00} = -\text{Gr } T_{00},$$

$$(2.20) \quad k_1 u_{01}''' + u_{01}'' + u_{01}' - M u_{01} = -\text{Gr } T_{01},$$

$$(2.21) \quad k_1 \left\{ u_{10}''' - \frac{i\omega}{4} u_{10}'' \right\} + u_{10}'' + u_{10}' - \left\{ M + \frac{i\omega}{4} \right\} u_{10} = -\text{Gr } T_{10},$$

$$(2.22) \quad k_1 \left\{ u_{11}''' - \frac{i\omega}{4} u_{11}'' \right\} + u_{11}'' + u_{11}' - \left\{ M + \frac{i\omega}{4} \right\} u_{11} = -\text{Gr } T_{11},$$

$$(2.23) \quad \beta_1 T_{00}'' + \text{Pr } T_{00}' - \frac{1}{4} \text{Pr } \phi T_{00} = 0,$$

$$(2.24) \quad \beta_1 T''_{01} + \text{Pr} T'_{01} - \frac{1}{4} \text{Pr} \phi T_{00} = -\text{Pr} (u'_{00})^2 - k_1 \text{Pr} u'_{00} u''_{00},$$

$$(2.25) \quad \beta_1 T''_{10} + \text{Pr} T'_{10} - \frac{1}{4} \text{Pr} (\phi - i\omega) T_{10} = 0,$$

$$(2.26) \quad \beta_1 T''_{11} + \text{Pr} T'_{11} - \frac{\text{Pr} (\phi - i\omega)}{4} T_{11} = -2 \text{Pr} u'_{00} u'_{10} \\ + k_1 \text{Pr} \left\{ \frac{i\omega}{4} u'_{00} u'_{10} - u'_{10} u''_{00} - u'_{00} u''_{10} \right\}.$$

The equivalent boundary conditions are

$$(2.27) \quad \left. \begin{aligned} u_{00} = 0, \quad u_{01} = 0, \quad u_{10} = 0, \quad u_{11} = 0 \\ T_{00} = 1, \quad T_{01} = 0, \quad T_{10} = 1, \quad T_{11} = 0 \end{aligned} \right\} \text{ at } y = 0,$$

$$\left. \begin{aligned} u_{00} \rightarrow 0, \quad u_{01} \rightarrow 0, \quad u_{10} \rightarrow 0, \quad u_{11} \rightarrow 0 \\ T_{00} \rightarrow 0, \quad T_{01} \rightarrow 0, \quad T_{10} \rightarrow 0, \quad T_{11} \rightarrow 0 \end{aligned} \right\} \text{ as } y \rightarrow \infty.$$

To solve Eqs (2.19) to (2.26), we consider very small values of k_1 so that the velocity and the temperature field can be expressed as:

$$(2.28) \quad \begin{aligned} u_{00} &= u_{000}(y) + k_1 u_{001}(y) + o(k_1^2), & T_{00} &= T_{000}(y) + k_1 T_{001}(y) + o(k_1^2), \\ u_{01} &= u_{010}(y) + k_1 u_{011}(y) + o(k_1^2), & T_{10} &= T_{100}(y) + k_1 T_{101}(y) + o(k_1^2), \\ u_{10} &= u_{100}(y) + k_1 u_{101}(y) + o(k_1^2), & T_{01} &= T_{010}(y) + k_1 T_{011}(y) + o(k_1^2), \\ u_{11} &= u_{110}(y) + k_1 u_{111}(y) + o(k_1^2), & T_{11} &= T_{110}(y) + k_1 T_{111}(y) + o(k_1^2). \end{aligned}$$

Substituting Eqs (2.28) into Eqs (2.19) to (2.26), we obtain the following sets of ordinary differential equations:

$$(2.29) \quad u''_{000} + u'_{000} - M u_{000} = -\text{Gr} T_{000},$$

$$(2.30) \quad u''_{001} + u'_{001} + u'_{001} - M u_{001} = u'''_{000} - \text{Gr} T_{001},$$

$$(2.31) \quad u''_{010} + u'_{010} - M u_{010} = -\text{Gr} T_{010},$$

$$(2.32) \quad u''_{011} + u'_{011} - M u_{011} = -u'''_{0110} - \text{Gr} T_{011},$$

$$(2.33) \quad u''_{100} + u'_{100} - \left\{ M + \frac{i\omega}{4} \right\} u_{100} = \text{Gr} T_{100},$$

$$(2.34) \quad u''_{101} + u'_{101} - \left\{ M + \frac{i\omega}{4} \right\} u_{101} = u'''_{100} + \frac{i\omega}{4} u''_{100} - \text{Gr} T_{101},$$

$$(2.35) \quad u''_{110} + u'_{110} - \left\{ M + \frac{i\omega}{4} \right\} u_{110} = \text{Gr } T_{110},$$

$$(2.36) \quad u''_{111} + u'_{111} - \left\{ M + \frac{i\omega}{4} \right\} u_{111} = -u'''_{110} + \frac{i\omega}{4} u''_{110} - \text{Gr } T_{111},$$

$$(2.37) \quad \beta_1 T''_{000} + \text{Pr } T'_{000} - \frac{1}{4} \text{Pr } \phi T_{000} = 0,$$

$$(2.38) \quad \beta_1 T''_{001} + \text{Pr } T'_{001} - \frac{1}{4} \text{Pr } \phi T_{001} = 0,$$

$$(2.39) \quad \beta_1 T''_{010} + \text{Pr } T'_{010} - \frac{1}{4} \text{Pr } \phi T_{010} = -\text{Pr } (u'_{000})^2,$$

$$(2.40) \quad \beta_1 T''_{011} + \text{Pr } T'_{011} - \frac{1}{4} \text{Pr } \phi T_{011} = -2 \text{Pr } u'_{000} u'_{001} - \text{Pr } u'_{000} u''_{000},$$

$$(2.41) \quad \beta_1 T''_{100} + \text{Pr } T'_{100} - \frac{1}{4} \text{Pr } (\phi - i\omega) T_{100} = 0,$$

$$(2.42) \quad \beta_1 T''_{101} + \text{Pr } T'_{101} - \frac{1}{4} \text{Pr } (\phi - i\omega) T_{101} = 0,$$

$$(2.43) \quad \beta_1 T''_{110} + \text{Pr } T'_{110} - \frac{1}{4} \text{Pr } (\phi - i\omega) T_{110} = -2 \text{Pr } u'_{000} u'_{100},$$

$$(2.44) \quad \beta_1 T''_{111} + \text{Pr } T'_{111} - \frac{1}{4} \text{Pr } (\phi - i\omega) T_{111} = -2 \text{Pr } (u'_{000} u'_{101} + u'_{100} u'_{001})$$

$$+ \left\{ \frac{i\omega}{4} u'_{000} u'_{100} - u'_{100} u''_{000} - u'_{000} u''_{100} \right\}.$$

The modified boundary conditions are as follows:

$$(2.45) \quad \left. \begin{array}{cccc} u_{000} = 0, & u_{001} = 0, & u_{010} = 0, & u_{011} = 0 \\ u_{100} = 0, & u_{101} = 0, & u_{110} = 0, & u_{111} = 0 \\ T_{000} = 1, & T_{001} = 0, & T_{100} = 1, & T_{101} = 0 \\ T_{010} = 1, & T_{011} = 0, & T_{110} = 1, & T_{111} = 0 \end{array} \right\} \text{ at } y = 0,$$

$$\left. \begin{array}{cccc} u_{000} \rightarrow 0, & u_{001} \rightarrow 0, & u_{010} \rightarrow 0, & u_{011} \rightarrow 0 \\ u_{100} \rightarrow 0, & u_{101} \rightarrow 0, & u_{110} \rightarrow 0, & u_{111} \rightarrow 0 \\ T_{000} \rightarrow 0, & T_{001} \rightarrow 0, & T_{100} \rightarrow 0, & T_{101} \rightarrow 0 \\ T_{010} \rightarrow 0, & T_{011} \rightarrow 0, & T_{110} \rightarrow 0, & T_{111} \rightarrow 0 \end{array} \right\} \text{ as } y \rightarrow \infty.$$

Solving the differential Eqs (2.29) to (2.44), subject to the boundary conditions (2.45), we get the solutions for velocity and temperature

$$u_{000} = A_1 e^{m_2 y} + A_2 e^{m_6 y},$$

$$u_{001} = A_3 e^{m_6 y} + A_4 e^{m_2 y} + A_5 e^{m_8 y},$$

$$u_{010} = A_6 e^{m_{10} y} + A_7 e^{2m_6 y} + A_8 e^{2m_2 y} + A_9 e^{(m_2+m_6)y} + A_{10} e^{m_{12} y},$$

$$\begin{aligned} u_{011} = & A_{11} e^{m_{12} y} + A_{12} e^{m_{10} y} + A_{13} e^{2m_6 y} + A_{14} e^{2m_2 y} + A_{15} e^{(m_2+m_6)y} \\ & + A_{16} e^{m_{14} y} + A_{17} e^{(m_2+m_8)y} + A_{18} e^{(m_2+m_6)y} + A_{19} e^{2m_2 y} + A_{20} e^{(m_8+m_6)y} \\ & + A_{21} e^{2m_6 y} + A_{22} e^{(m_2+m_6)y} + A_{23} e^{2m_2 y} + A_{24} e^{(m_2+m_6)y} \\ & + A_{25} e^{(m_2+m_6)y} + A_{26} e^{2m_6 y} + A_{27} e^{m_{16} y}, \end{aligned}$$

$$u_{100} = Z_1 e^{m_1 y},$$

$$u_{101} = Z_2 e^{m_1 y} + Z_3 e^{m_1 y},$$

$$u_{110} = A_{28} e^{(m_1+m_2)y} + A_{29} e^{(m_1+m_2)y} + A_{30} e^{m_7 y} + A_{31} e^{m_9 y},$$

$$\begin{aligned} u_{111} = & A_{32} e^{m_9 y} + A_{33} e^{(m_1+m_2)y} + A_{34} e^{(m_1+m_2)y} + A_{35} e^{m_7 y} + A_{36} e^{m_9 y} \\ & + A_{37} e^{(m_1+m_2)y} + A_{38} e^{(m_1+m_2)y} + A_{39} e^{m_7 y} + A_{40} e^{m_9 y} + A_{41} e^{(m_1+m_2)y} \\ & + A_{42} e^{(m_1+m_2)y} + A_{43} e^{(m_1+m_2)y} + A_{44} e^{(m_1+m_2)y} + A_{45} e^{(m_1+m_6)y} \\ & + A_{46} e^{(m_1+m_2)y} + A_{47} e^{(m_1+m_8)y} + A_{48} e^{(m_1+m_2)y} + A_{49} e^{(m_1+m_6)y} \\ & + A_{50} e^{(m_1+m_2)y} + A_{51} e^{(m_1+m_6)y} + A_{52} e^{(m_1+m_6)y} + A_{53} e^{m_9 y}, \end{aligned}$$

$$T_{000} = e^{m_2 y},$$

$$T_{001} = 0,$$

$$T_{010} = B_1 e^{2m_6 y} + B_2 e^{2m_2 y} + B_3 e^{(m_2+m_6)y} + B_4 e^{m_{10} y},$$

$$\begin{aligned} T_{011} = & B_5 e^{(m_2+m_8)y} + B_6 e^{(m_2+m_6)y} + B_7 e^{2m_2 y} + B_8 e^{(m_6+m_8)y} + B_9 e^{2m_6 y} \\ & + B_{10} e^{(m_2+m_6)y} + B_{11} e^{2m_2 y} + B_{12} e^{(m_2+m_6)y} + B_{13} e^{(m_2+m_6)y} \\ & + B_{14} e^{2m_6 y} + B_{15} e^{m_{14} y}, \end{aligned}$$

$$T_{100} = e^{m_1 y},$$

$$T_{101} = 0,$$

$$T_{110} = B_{16} e^{(m_1+m_2)y} + B_{17} e^{(m_1+m_2)y} + B_{18} e^{m_7 y},$$

$$\begin{aligned}
 T_{111} = & B_{19}e^{(m_1+m_2)y} + B_{20}e^{(m_1+m_2)y} + B_{21}e^{(m_1+m_2)y} + B_{22}e^{(m_1+m_2)y} \\
 & + B_{23}e^{(m_1+m_6)y} + B_{24}e^{(m_1+m_2)y} + B_{25}e^{(m_1+m_8)y} + B_{26}e^{(m_1+m_2)y} \\
 & + B_{27}e^{(m_1+m_6)y} + B_{28}e^{(m_1+m_2)y} + B_{29}e^{(m_1+m_6)y} + B_{30}e^{(m_1+m_2)y} \\
 & + B_{31}e^{(m_2+m_6)y} + B_{32}e^{m_9y}.
 \end{aligned}$$

In view of the above, Eq. (2.28) then becomes

$$\begin{aligned}
 u_0 = & A_1e^{m_2y} + A_2e^{m_6y} + k_1 (A_3e^{m_6y} + A_4e^{m_2y} + A_5e^{m_8y}) \\
 & + Ec \left[A_6e^{m_{10}y} + A_7e^{2m_6y} + A_8e^{2m_2y} + A_9e^{(m_2+m_6)y} + A_{10}e^{m_{12}y} \right. \\
 & + k_1 \{ A_{11}e^{m_{12}y} + A_{12}e^{m_{10}y} + A_{13}e^{2m_6y} + A_{14}e^{2m_2y} + A_{15}e^{(m_2+m_6)y} \\
 & + A_{16}e^{m_{14}y} + A_{17}e^{(m_2+m_8)y} + A_{18}e^{(m_2+m_6)y} + A_{19}e^{2m_2y} + A_{20}e^{(m_8+m_6)y} \\
 & + A_{21}e^{2m_6y} + A_{22}e^{(m_2+m_6)y} + A_{23}e^{2m_2y} + A_{24}e^{(m_2+m_6)y} + A_{25}e^{(m_2+m_6)y} \\
 & \left. + A_{26}e^{2m_6y} + A_{27}e^{m_{16}y} \right\}],
 \end{aligned}$$

$$\begin{aligned}
 T_0 = & e^{m_2y} + Ec \left[B_1e^{2m_6y} + B_2e^{2m_2y} + B_3e^{(m_2+m_6)y} + B_4e^{m_{10}y} + k_1 \left\{ B_5e^{(m_2+m_8)y} \right. \right. \\
 & + B_6e^{(m_2+m_6)y} + B_7e^{2m_2y} + B_8e^{(m_6+m_8)y} + B_9e^{2m_6y} + B_{10}e^{(m_2+m_6)y} \\
 & \left. \left. + B_{11}e^{2m_2y} + B_{12}e^{(m_2+m_6)y} + B_{13}e^{(m_2+m_6)y} + B_{14}e^{2m_6y} + B_{15}e^{m_{14}y} \right\} \right],
 \end{aligned}$$

$$\begin{aligned}
 u_1 = & C_1e^{m_1y} + k_1 (C_2e^{m_1y} + C_3e^{m_1y}) + Ec \left\{ A_{28}e^{(m_1+m_2)y} + A_{29}e^{(m_1+m_2)y} \right. \\
 & + A_{30}e^{m_7y} + A_{31}e^{m_9y} + k_1 \left(A_{32}e^{m_9y} + A_{33}e^{(m_1+m_2)y} + A_{34}e^{(m_1+m_2)y} \right. \\
 & + A_{35}e^{m_7y} + A_{36}e^{m_9y} + A_{37}e^{(m_1+m_2)y} + A_{38}e^{(m_1+m_2)y} + A_{39}e^{m_7y} \\
 & + A_{40}e^{m_9y} + A_{41}e^{(m_1+m_2)y} + A_{42}e^{(m_1+m_2)y} + A_{43}e^{(m_1+m_2)y} \\
 & + A_{44}e^{(m_1+m_2)y} + A_{45}e^{(m_1+m_6)y} + A_{46}e^{(m_1+m_2)y} + A_{47}e^{(m_1+m_8)y} \\
 & + A_{48}e^{(m_1+m_2)y} + A_{49}e^{(m_1+m_6)y} + A_{50}e^{(m_1+m_2)y} + A_{51}e^{(m_1+m_6)y} \\
 & \left. \left. + A_{52}e^{(m_1+m_6)y} + A_{53}e^{m_9y} \right) \right\},
 \end{aligned}$$

$$\begin{aligned}
 T_1 = & e^{m_1y} + Ec \left\{ B_{16}e^{(m_1+m_2)y} + B_{17}e^{(m_1+m_2)y} + B_{18}e^{m_7y} + k_1 \left(B_{19}e^{(m_1+m_2)y} \right. \right. \\
 & + B_{20}e^{(m_1+m_2)y} + B_{21}e^{(m_1+m_2)y} + B_{22}e^{(m_1+m_2)y} + B_{23}e^{(m_1+m_6)y} \\
 & + B_{24}e^{(m_1+m_2)y} + B_{25}e^{(m_1+m_8)y} + B_{26}e^{(m_1+m_2)y} + B_{27}e^{(m_1+m_6)y} \\
 & + B_{28}e^{(m_1+m_2)y} + B_{29}e^{(m_1+m_6)y} + B_{30}e^{(m_1+m_2)y} \\
 & \left. \left. + B_{31}e^{(m_2+m_6)y} + B_{32}e^{m_9y} \right) \right\}.
 \end{aligned}$$

In view of the above, Eq. (2.12) becomes

$$\begin{aligned}
 u(y, t) = \varepsilon e^{i\omega t} & \left\{ C_1 e^{m_1 y} + k_1 (C_2 e^{m_1 y} + C_3 e^{m_1 y}) + \text{Ec} \left\{ A_{28} e^{(m_1+m_2)y} \right. \right. \\
 & + A_{29} e^{(m_1+m_2)y} + A_{30} e^{m_7 y} + A_{31} e^{m_9 y} + k_1 \left(A_{32} e^{m_9 y} + A_{33} e^{(m_1+m_2)y} \right. \\
 & + A_{34} e^{(m_1+m_2)y} + A_{35} e^{m_7 y} + A_{36} e^{m_9 y} + A_{37} e^{(m_1+m_2)y} + A_{38} e^{(m_1+m_2)y} \\
 & + A_{39} e^{m_7 y} + A_{40} e^{m_9 y} + A_{41} e^{(m_1+m_2)y} + A_{42} e^{(m_1+m_2)y} + A_{43} e^{(m_1+m_2)y} \\
 & + A_{44} e^{(m_1+m_2)y} + A_{45} e^{(m_1+m_6)y} + A_{46} e^{(m_1+m_2)y} + A_{47} e^{(m_1+m_8)y} \\
 & + A_{48} e^{(m_1+m_2)y} + A_{49} e^{(m_1+m_6)y} + A_{50} e^{(m_1+m_2)y} + A_{51} e^{(m_1+m_6)y} \\
 & \left. \left. + A_{52} e^{(m_1+m_6)y} + A_{53} e^{m_9 y} \right) \right\} + \left\{ A_1 e^{m_2 y} + A_2 e^{m_6 y} + k_1 (A_3 e^{m_6 y} \right. \\
 & + A_4 e^{m_2 y} + A_5 e^{m_8 y}) + \text{Ec} \left[A_6 e^{m_{10} y} + A_7 e^{2m_6 y} + A_8 e^{2m_2 y} + A_9 e^{(m_2+m_6)y} \right. \\
 & + A_{10} e^{m_{12} y} + k_1 \left\{ A_{11} e^{m_{12} y} + A_{12} e^{m_{10} y} + A_{13} e^{2m_6 y} + A_{14} e^{2m_2 y} \right. \\
 & + A_{15} e^{(m_2+m_6)y} + A_{16} e^{m_{14} y} + A_{17} e^{(m_2+m_8)y} + A_{18} e^{(m_2+m_6)y} + A_{19} e^{2m_2 y} \\
 & + A_{20} e^{(m_8+m_6)y} + A_{21} e^{2m_6 y} + A_{22} e^{(m_2+m_6)y} + A_{23} e^{2m_2 y} + A_{24} e^{(m_2+m_6)y} \\
 & \left. \left. + A_{25} e^{(m_2+m_6)y} + A_{26} e^{2m_6 y} + A_{27} e^{m_{16} y} \right\} \right] \left. \right\},
 \end{aligned}$$

$$\begin{aligned}
 T(y, t) = \varepsilon e^{i\omega t} & \left\{ e^{m_1 y} + \text{Ec} \left\{ B_{16} e^{(m_1+m_2)y} + B_{17} e^{(m_1+m_2)y} + B_{18} e^{m_7 y} \right. \right. \\
 & + k_1 \left(B_{19} e^{(m_1+m_2)y} + B_{20} e^{(m_1+m_2)y} + B_{21} e^{(m_1+m_2)y} + B_{22} e^{(m_1+m_2)y} \right. \\
 & + B_{23} e^{(m_1+m_6)y} + B_{24} e^{(m_1+m_2)y} + B_{25} e^{(m_1+m_8)y} + B_{26} e^{(m_1+m_2)y} \\
 & + B_{27} e^{(m_1+m_6)y} + B_{28} e^{(m_1+m_2)y} + B_{29} e^{(m_1+m_6)y} + B_{30} e^{(m_1+m_2)y} \\
 & \left. \left. + B_{31} e^{(m_2+m_6)y} + B_{32} e^{m_9 y} \right) \right\} + \left\{ e^{m_2 y} + \text{Ec} \left[B_1 e^{2m_6 y} + B_2 e^{2m_2 y} \right. \right. \\
 & + B_3 e^{(m_2+m_6)y} + B_4 e^{m_{10} y} + k_1 \left\{ B_5 e^{(m_2+m_8)y} + B_6 e^{(m_2+m_6)y} + B_7 e^{2m_2 y} \right. \\
 & + B_8 e^{(m_6+m_8)y} + B_9 e^{2m_6 y} + B_{10} e^{(m_2+m_6)y} + B_{11} e^{2m_2 y} + B_{12} e^{(m_2+m_6)y} \\
 & \left. \left. + B_{13} e^{(m_2+m_6)y} + B_{14} e^{2m_6 y} + B_{15} e^{m_{14} y} \right\} \right] \left. \right\}.
 \end{aligned}$$

The skin friction coefficient C_f is given as:

$$\begin{aligned}
 C_f = \left(\frac{\partial u}{\partial y} \right)_{y=0} &= \varepsilon e^{i\omega t} \left\{ C_1 m_1 + k_1 (C_2 + C_3) m_1 + \text{Ec} \left\{ (A_{28} + A_{29})(m_1 + m_2) \right. \right. \\
 &+ A_{30} m_7 + A_{31} m_9 + k_1 \left((A_{33} + A_{34} + A_{37} + A_{38} + A_{41} + A_{42} + A_{43} + A_{44} \right. \\
 &+ A_{46} + A_{48} + A_{50})(m_1 + m_2) + (A_{35} + A_{37}) m_7 + (A_{32} + A_{36} + A_{39} + A_{40} \\
 &\left. \left. + A_{53}) m_9 + (A_{45} + A_{49} + A_{51} + A_{52})(m_1 + m_6) + A_{47}(m_1 + m_8) \right\} \right\} \\
 &+ \left\{ A_1 m_2 + A_2 m_6 + k_1 (A_3 m_6 + A_4 m_2 + A_5 m_8) + \text{Ec} \left[A_6 m_{10} + 2A_7 m_6 + 2A_8 m_2 \right. \right. \\
 &+ A_9 (m_2 + m_6) + A_{10} m_{12} + k_1 \left\{ A_{11} m_{12} + A_{12} m_{10} + 2(A_{13} + A_{21} + A_{26}) m_6 \right. \\
 &+ 2(A_{14} + A_{19} + A_{23}) m_2 + (A_{15} + A_{18} + A_{22} + A_{24} + A_{25})(m_2 + m_6) \\
 &\left. \left. \left. + A_{16} m_{14} + A_{17}(m_2 + m_8) + A_{20}(m_6 + m_8) + A_{27} m_{16} \right\} \right] \right\}.
 \end{aligned}$$

The heat transfer rate in terms of Nusselt number is given as:

$$\begin{aligned}
 \text{Nu} = \left(\frac{\partial T}{\partial y} \right)_{y=0} &= \varepsilon e^{i\omega t} \left\{ m_1 + \text{Ec} \left\{ (B_{16} + B_{17})(m_1 + m_2) + B_{18} m_7 \right. \right. \\
 &+ k_1 \left((B_{19} + B_{20} + B_{21} + B_{22} + B_{24} + B_{26} + B_{28} + B_{30})(m_1 + m_2) \right. \\
 &\left. \left. + (B_{23} + B_{27} + B_{29})(m_1 + m_6) + B_{25}(m_1 + m_8) + B_{31}(m_2 + m_6) + B_{32} m_9 \right\} \right\} \\
 &+ \left\{ m_2 + \text{Ec} \left[2B_1 m_6 + 2B_2 m_2 + B_3 (m_2 + m_6) + B_4 m_{10} + k_1 \left\{ (B_6 + B_{10} + B_{12} + B_{13}) \right. \right. \right. \\
 &\left. \left. (m_2 + m_6) + B_5 (m_2 + m_8) + 2(B_7 + B_{11}) m_2 + B_8 (m_6 + m_8) \right. \right. \\
 &\left. \left. \left. + 2(B_9 + B_{14}) m_6 + B_{15} m_{14} \right\} \right] \right\}.
 \end{aligned}$$

3. RESULTS AND DISCUSSION

The purpose of this study is to present the effects of non-Newtonian parameter on the unsteady MHD flow. Additionally, heat transfer characteristics as the effects of other parameters are discussed. Figures 1 to 6 represent the velocity (u) and temperature (T) profiles against y for various values of the Eckert number Ec , the Grashof number Gr , the Hartmann number M , the radiation parameter N , the heat source parameter Q , and the Prandtl number Pr for both the Newtonian and non-Newtonian cases. Further, the non-Newtonian effect is

exhibited through the non-dimensional parameter k_1 . The corresponding result of Newtonian fluid is obtained by setting $k_1 = 0$. It is worth mentioning that these results coincide with the results obtained by SAHOO *et al.* [5] (Tables 1 and 2 depict the magnetic field values for the shear stress and the radiation parameter for the heat transfer rate. It is clear that the shear stress increases while the heat transfer rate decreases with the increasing value of the non-Newtonian parameter k_1 compared with the Newtonian fluid for different values).

Table 1. The shear stress for different values of magnetic field.

M	$k_1 = 0$		$k_1 = 0.02$		$k_1 = 0.04$	
	CHOUDHURY, DEY [38]	Present study	CHOUDHURY, DEY [38]	Present study	CHOUDHURY, DEY [38]	Present study
0.5	4.5312	4.86568	5.4147	5.53129	7.0162	7.98745
1.0	5.9017	5.45638	6.6149	6.90173	8.4562	8.56439
1.5	6.5601	6.89656	7.7206	8.16016	9.8214	9.12568
2.0	7.0548	7.15436	8.8283	9.05485	10.2073	10.3567

Table 2. The heat transfer rate for different values of radiation.

N	$k_1 = 0$		$k_1 = 0.02$		$k_1 = 0.04$	
	CHOUDHURY, DEY [38]	Present study	CHOUDHURY, DEY [38]	Present study	CHOUDHURY, DEY [38]	Present study
0.2	3.5312	3.534257	5.8147	5.813875	7.0162	7.115842
0.4	2.9017	2.917746	4.5149	4.525890	6.4562	6.467392
0.6	2.5601	2.560834	3.8206	3.821743	5.8214	5.835914
0.8	2.0548	2.055962	3.2283	3.235972	5.2073	5.216073

The Eckert number Ec expresses the relationship between the kinetic energy in the flow and the enthalpy. It embodies the conversion of kinetic energy into internal energy by work done against the viscous fluid stress. Figure 1 illustrate the effect of Ec (i.e., viscous dissipation effect) on the velocity and temperature profiles, respectively. It is clear that both the fluid profiles u and T increase with variations of Ec . The Eckert number expresses the relation between the kinetic energy in the flow and the enthalpy. It embodies the conversion of kinetic energy into internal energy by work done against viscous fluid stresses. This is caused by the increase in the kinetic energy caused by viscous dissipation in the boundary layer, which leads to a small temperature gradient. Therefore, the fluid temperature increases the thermal buoyancy effects, which induces more flow along the path. Further, Ec implies that the kinetic energy is large, resulting in an increased vibration of the fluid leading to an increased collision of the fluid molecules and increases the dissipation of heat in the boundary layer region

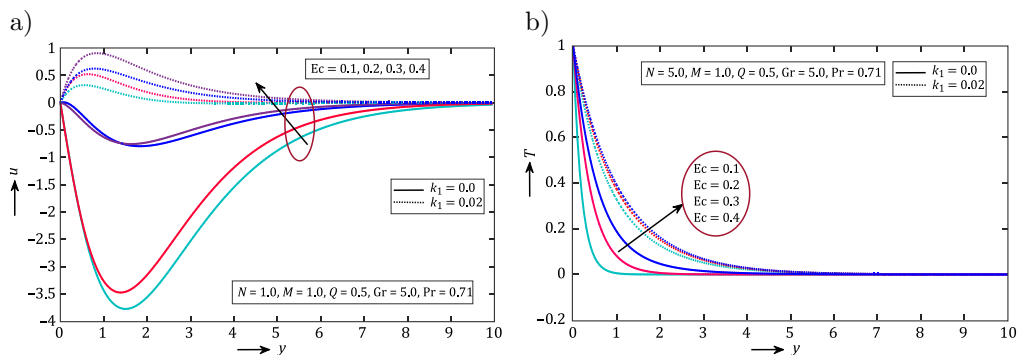


FIG. 1. Velocity (a) and temperature (b) profiles for different values of Ec .

hence an increase in T is observed. Interestingly, it is also noticed that the thermal boundary layer thickness is increased in the presence of viscous dissipation.

Figure 2 shows that the velocity rises steeply near the vertical wall as Gr is increased. The fluid moving away from the wall, across-flow in the velocity is induced and turns to zero at a slower rate for small Gr . Hence, the velocity and thermal boundary reduce as Gr increases, causing the fluid temperature to reduce at every point other than the wall.

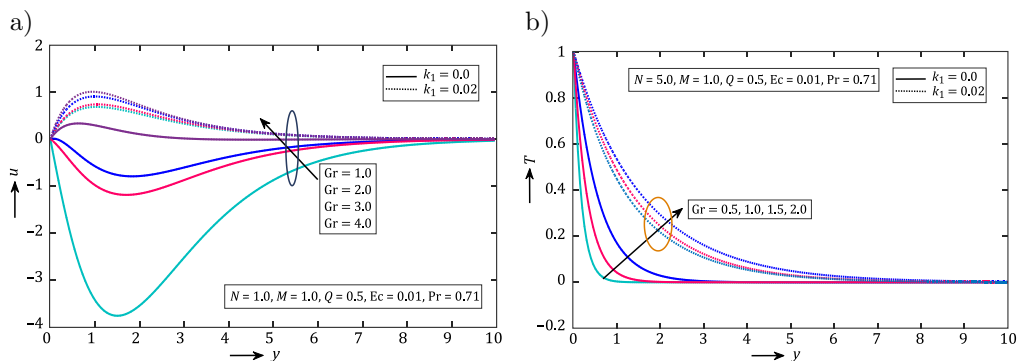


FIG. 2. Velocity (a) and temperature (b) profiles for different values of Gr .

The effect of the magnetic field parameter M on the velocity and temperature profiles for both the Newtonian and non-Newtonian cases is shown in Fig. 3. It is observed that in both the cases (i.e., $k_1 = 0$ and $k_1 \neq 0$), the fluid velocity and temperature increased with increasing of M . Thus, the presence of a Hartmann number generates a Lorentz force, which diminishes the velocity field, while it enhances the temperature of the fluid. Moreover, from the physical point of view, the Lorentz force increases and an increase of the magnetic field becomes stronger, which ultimately slows down the fluid flow and increases the temperature.

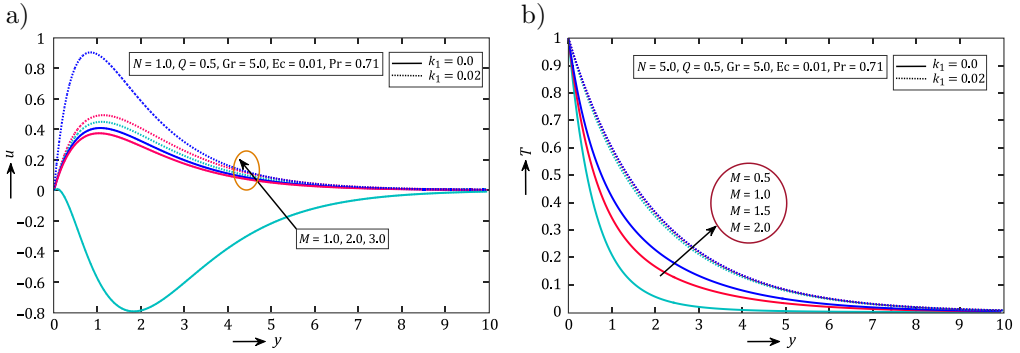


FIG. 3. Velocity (a) and temperature (b) profiles for different values of M .

Figure 4 shows the velocity and temperature profiles for different values of N . Increasing the radiation parameter N produces significant decreases in the thermal condition of the fluid temperature, which consequently induces more fluid in the boundary layer through buoyancy effect causing the velocity in the fluid to decrease. Further, both the hydromagnetic boundary layer and thermal boundary layer thicknesses were observed to decrease as a result of increasing N .

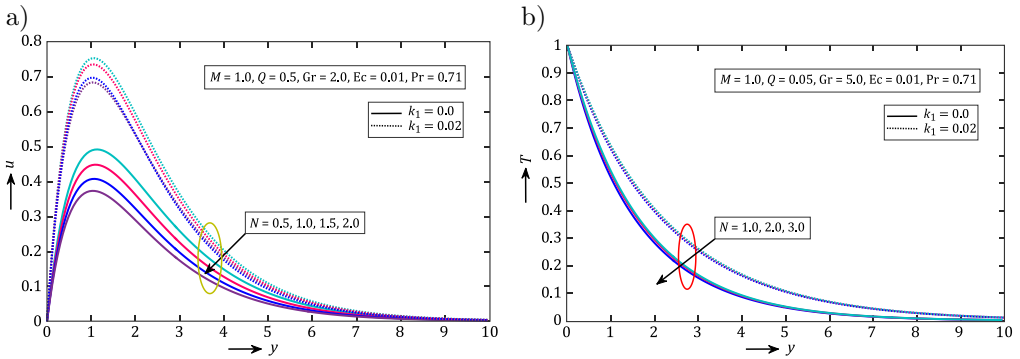


FIG. 4. Velocity (a) and temperature (b) profiles for different values of N .

The Prandtl number Pr is defined as the ratio of momentum diffusivity to thermal diffusivity. Figure 5 shows the behavior of velocity and temperature for different values of Pr . It is observed in Fig. 5a that an increase in the Pr means a slow rate of thermal diffusion for the non-Newtonian fluid, but the opposite effect is observed for the Newtonian fluid. Further, it is observed that an increase in Pr causes a decrease of the thermal boundary layer thickness. The reason is that smaller values of Pr are equivalent to an increase in the thermal conductivity of the fluid. Therefore, heat is able to diffuse away from the heated surface

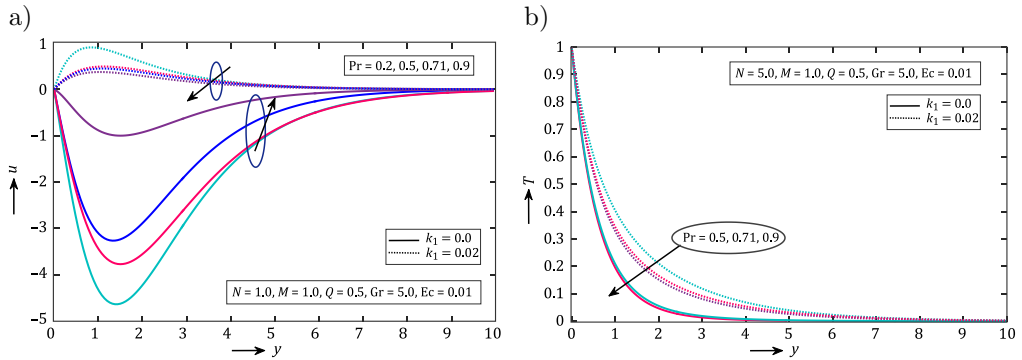


FIG. 5. Velocity (a) and temperature (b) profiles for different values of Pr.

more rapidly for higher values of Pr. In heat transfer problems, the Prandtl number controls the relative thickening of momentum and thermal boundary layers. When the Prandtl number is small, it means that heat diffuses quickly compared to the velocity (momentum), which means that for liquid metals, the thickness of the thermal boundary layer is much bigger than the momentum boundary layer. Hence, the Prandtl number can be used to increase the rate of cooling in conducting flows.

The influence of heat source parameter Q on the fluid velocity and temperature profiles is displayed, respectively, in Figs. 6a and 6b. The fluid velocity rises with increasing values of Q . Further, it is noted for these plots that the temperature of the fluid decreases with an increase in Q . It is also observed that the magnitude in the case Q is larger compared with the case when the heat source is present in the system. Therefore, we can conclude that the heat enhancement phenomenon can be controlled very efficiently by adding the heat source into the system. This result is very significant for the flow in which the heat transfer is given an utmost importance.

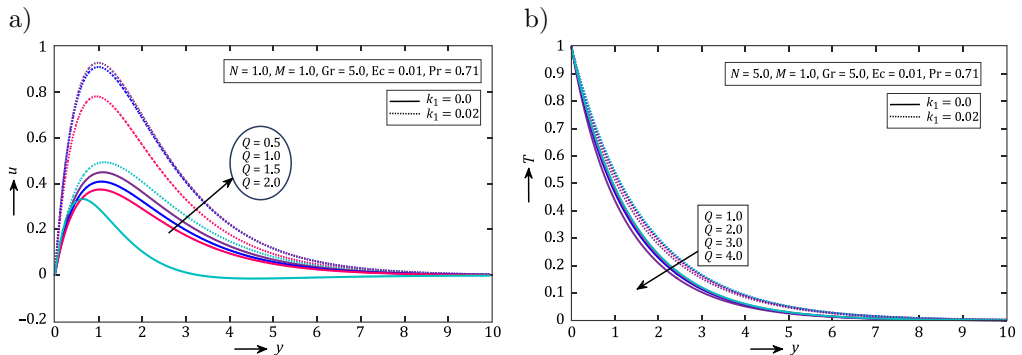


FIG. 6. Velocity (a) and temperature (b) profiles for different values of Q .

4. CONCLUSIONS

The presented analysis produced the following results for the velocity and temperature profiles of the flow field:

- (i) Velocity rises steeply near the vertical wall as the Grashof number is increased.
- (ii) For both the Newtonian and non-Newtonian cases, the fluid profiles of velocity (u) and (T) increase with increasing Prandtl and Eckert numbers and magnetic field parameter.
- (iii) The fluid velocity increases while the fluid temperature decreases with the increase of the heat source parameter.
- (iv) Increasing the radiation parameter produces significant decreases in the velocity and thermal condition of the fluid temperature.

Highlights

- Energy conversion is an application for thermal systems.
- Thermal energy enhancement is observed for various values of relevant parameters.
- The results are examined and compared with other studies.

APPENDIX

$$\begin{aligned}
 m_1 &= -\frac{\text{Pr} + \sqrt{\text{Pr}^2 + \beta_1 \text{Pr}(\phi - i\omega)}}{2\beta_1}, & m_2 &= -\frac{\text{Pr} + \sqrt{\text{Pr}^2 + \beta_1 \text{Pr} \phi}}{2\beta_1}, \\
 m_3 &= -\left(1 + \sqrt{1 + 4M + i\omega}\right)/2, & m_4 &= -\frac{\text{Pr} + \sqrt{\text{Pr}^2 + \beta_1 \text{Pr} \phi}}{2\beta_1}, \\
 m_5 &= -\frac{\text{Pr} + \sqrt{\text{Pr}^2 + \beta_1 \text{Pr}(\phi - i\omega)}}{2\beta_1}, & m_6 &= -(1 + \sqrt{1 + 4M})/2, \\
 m_7 &= -\frac{\text{Pr} + \sqrt{\text{Pr}^2 + \beta_1 \text{Pr}(\phi - i\omega)}}{2\beta_1}, & m_8 &= -(1 + \sqrt{1 + 4M})/2, \\
 m_9 &= -\frac{\text{Pr} + \sqrt{\text{Pr}^2 + \beta_1 \text{Pr}(\phi - i\omega)}}{2\beta_1}, & m_{10} &= -\frac{\text{Pr} + \sqrt{\text{Pr}^2 + \beta_1 \text{Pr} \phi}}{2\beta_1}, \\
 m_{11} &= -\left(1 + \sqrt{1 + 4M + i\omega}\right)/2, & m_{12} &= -(1 + \sqrt{1 + 4M})/2,
 \end{aligned}$$

$$\begin{aligned}
 m_{14} &= -\frac{\text{Pr} + \sqrt{\text{Pr}^2 + \beta_1 \text{Pr} \phi}}{2\beta_1}, & m_{16} &= -(1 + \sqrt{1 + 4M})/2, \\
 A_1 &= \frac{-\text{Gr}}{m_2^2 + m_2 - M}, & A_2 &= -A_1, \\
 A_3 &= \frac{-A_2 m_6^3}{m_6^2 + m_6 - M}, & A_4 &= \frac{-A_1 m_2^3}{m_2^2 + m_2 - M}, \\
 A_5 &= -(A_3 + A_4), & A_6 &= \frac{-\text{Gr} B_4}{m_{10}^2 - m_{10} - M}, \\
 A_7 &= -\frac{\text{Gr} B_1}{4m_6^2 + 2m_6 - M}, & A_8 &= \frac{-\text{Gr} B_2}{4m_2^2 + 2m_2 - M}, \\
 A_9 &= \frac{-\text{Gr} B_3}{(m_2 + m_6)^2 + m_2 + m_6 - M}, & A_{10} &= -(A_6 + A_7 + A_8 + A_9), \\
 A_{11} &= \frac{-A_{10} m_{12}^3}{m_{12}^2 + m_{12} - M}, & A_{12} &= \frac{-A_6 m_{10}^3}{m_{10}^2 + m_{10} - M}, \\
 A_{13} &= \frac{-8A_7 m_6^3}{4m_6^2 + 2m_6 - M}, & A_{14} &= \frac{-8A_8 m_2^3}{4m_2^2 + 2m_2 - M}, \\
 A_{15} &= \frac{-A_9 (m_2 + m_6)^3}{(m_2 + m_6)^2 + m_2 + m_6 - M}, & A_{16} &= \frac{-B_{15}}{m_{14}^2 + m_{14} - M}, \\
 A_{17} &= \frac{-B_5}{(m_2 + m_8)^2 + m_2 + m_8 - M}, & A_{18} &= \frac{-B_6}{(m_2 + m_6)^2 + m_2 + m_6 - M}, \\
 A_{19} &= \frac{-B_7}{4m_2^2 + 2m_2 - M}, & A_{20} &= \frac{-B_8}{(m_6 + m_8)^2 + m_6 + m_8 - M}, \\
 A_{21} &= \frac{-B_9}{4m_6^2 + 2m_6 - M}, & A_{22} &= \frac{-B_{10}}{(m_2 + m_6)^2 + m_2 + m_6 - M}, \\
 A_{23} &= \frac{-B_{11}}{4m_2^2 + 2m_2 - M}, & A_{24} &= \frac{-B_{12}}{(m_2 + m_6)^2 + m_2 + m_6 - M}, \\
 A_{25} &= \frac{-B_{13}}{(m_2 + m_6)^2 + m_2 + m_6 - M}, & A_{26} &= \frac{-B_{14}}{4m_6^2 + 2m_6 - M}, \\
 A_{27} &= -(A_{11} + A_{12} + A_{13} + A_{14} + A_{15} + A_{16} + A_{17} + A_{18} + A_{19} + A_{20} \\
 & \quad + A_{21} + A_{22} + A_{23} + A_{24} + A_{25} + A_{26}),
 \end{aligned}$$

$$A_{28} = \frac{\text{Gr}B_{16}}{(m_1 + m_2)^2 + (m_1 + m_2) - (M + \frac{i\omega}{4})},$$

$$A_{29} = \frac{\text{Gr}B_{17}}{(m_1 + m_2)^2 + (m_1 + m_2) - (M + \frac{i\omega}{4})},$$

$$A_{30} = \frac{\text{Gr}B_{18}}{m_7^2 + m_7 - (M + \frac{i\omega}{4})},$$

$$A_{31} = -(A_{28} + A_{29} + A_{30}),$$

$$A_{32} = -\frac{A_{31}m_9^3}{m_9^2 + m_9 - (M + \frac{i\omega}{4})},$$

$$A_{33} = -\frac{A_{28}(m_1 + m_2)^3}{(m_1 + m_2)^2 + (m_1 + m_2) - (M + \frac{i\omega}{4})},$$

$$A_{34} = -\frac{A_{29}(m_1 + m_2)^3}{(m_1 + m_2)^2 + (m_1 + m_2) - (M + \frac{i\omega}{4})},$$

$$A_{35} = -\frac{A_{30}m_7^3}{m_7^2 + m_7 - (M + \frac{i\omega}{4})},$$

$$A_{36} = \frac{1}{4} \frac{i\omega A_{31}m_9^2}{m_9^2 + m_9 - (M + \frac{i\omega}{4})},$$

$$A_{37} = \frac{1}{4} \frac{i\omega A_{28}(m_1 + m_2)^2}{(m_1 + m_2)^2 + (m_1 + m_2) - (M + \frac{i\omega}{4})},$$

$$A_{38} = \frac{1}{4} \frac{i\omega A_{29}(m_1 + m_2)^2}{(m_1 + m_2)^2 + (m_1 + m_2) - (M + \frac{i\omega}{4})},$$

$$A_{39} = \frac{1}{4} \frac{i\omega A_{30}m_7^2}{m_7^2 + m_7 - (M + \frac{i\omega}{4})},$$

$$A_{40} = -\frac{\text{Gr}B_{31}}{m_9^2 + m_9 - (M + \frac{i\omega}{4})},$$

$$A_{41} = -\frac{\text{Gr}B_{19}}{(m_1 + m_2)^2 + (m_1 + m_2) - (M + \frac{i\omega}{4})},$$

$$A_{42} = -\frac{\text{Gr}B_{20}}{(m_1 + m_2)^2 + (m_1 + m_2) - (M + \frac{i\omega}{4})},$$

$$A_{43} = -\frac{\text{Gr } B_{21}}{(m_1 + m_2)^2 + (m_1 + m_2) - \left(M + \frac{i\omega}{4}\right)},$$

$$A_{44} = -\frac{\text{Gr } B_{22}}{(m_1 + m_2)^2 + (m_1 + m_2) - \left(M + \frac{i\omega}{4}\right)},$$

$$A_{45} = -\frac{\text{Gr } B_{23}}{(m_1 + m_6)^2 + (m_1 + m_6) - \left(M + \frac{i\omega}{4}\right)},$$

$$A_{46} = -\frac{\text{Gr } B_{24}}{(m_1 + m_2)^2 + (m_1 + m_2) - \left(M + \frac{i\omega}{4}\right)},$$

$$A_{47} = -\frac{\text{Gr } B_{25}}{(m_1 + m_8)^2 + (m_1 + m_8) - \left(M + \frac{i\omega}{4}\right)},$$

$$A_{48} = -\frac{\text{Gr } B_{26}}{(m_1 + m_2)^2 + (m_1 + m_2) - \left(M + \frac{i\omega}{4}\right)},$$

$$A_{49} = -\frac{\text{Gr } B_{27}}{(m_1 + m_6)^2 + (m_1 + m_6) - \left(M + \frac{i\omega}{4}\right)},$$

$$A_{50} = -\frac{\text{Gr } B_{28}}{(m_1 + m_2)^2 + (m_1 + m_2) - \left(M + \frac{i\omega}{4}\right)},$$

$$A_{51} = -\frac{\text{Gr } B_{29}}{(m_1 + m_6)^2 + (m_1 + m_6) - \left(M + \frac{i\omega}{4}\right)},$$

$$A_{52} = -\frac{\text{Gr } B_{30}}{(m_1 + m_2)^2 + (m_1 + m_2) - \left(M + \frac{i\omega}{4}\right)},$$

$$A_{53} = -\frac{\text{Gr } B_{31}}{(m_2 + m_6)^2 + (m_2 + m_6) - \left(M + \frac{i\omega}{4}\right)},$$

$$A_{54} = -\frac{\text{Gr } B_{32}}{m_9^2 + m_9 - \left(M + \frac{i\omega}{4}\right)},$$

$$A_{55} = -(A_{32} + A_{33} + A_{34} + A_{35} + A_{36} + A_{37} + A_{38} + A_{39} + A_{40} + A_{41} + A_{42} + A_{43} + A_{44} + A_{45} + A_{46} + A_{47} + A_{48} + A_{49} + A_{50} + A_{51} + A_{52} + A_{53} + A_{54}),$$

$$B_1 = \frac{-4A_2^2 \text{Pr } m_6^3}{16\beta_1 m_6^2 + 8 \text{Pr } m_6 - \text{Pr } \varphi},$$

$$B_2 = \frac{-4A_1^2 \text{Pr } m_2^3}{16\beta_1 m_2^2 + 8 \text{Pr } m_2 - \text{Pr } \varphi},$$

$$B_3 = \frac{-8A_1A_2 \Pr m_2m_6}{4\beta_1(m_2 + m_6)^2 + 8 \Pr(m_2 + m_6) - \Pr \varphi},$$

$$B_4 = -(B_1 + B_2 + B_3),$$

$$B_5 = \frac{-8A_1A_5 \Pr m_2m_8}{4\beta_1(m_2 + m_8)^2 + 4 \Pr(m_2 + m_8) - \Pr \varphi},$$

$$B_6 = \frac{-8A_1A_3 \Pr m_2m_6}{4\beta_1(m_2 + m_6)^2 + 4 \Pr(m_2 + m_6) - \Pr \varphi},$$

$$B_7 = \frac{-8A_1A_4 \Pr m_2^2}{16\beta_1m_2^2 + 8 \Pr m_2 - \Pr \varphi},$$

$$B_8 = \frac{-8A_2A_5 \Pr m_8m_6}{4\beta_1(m_8 + m_6)^2 + 4 \Pr(m_8 + m_6) - \Pr \varphi},$$

$$B_9 = \frac{-8A_2A_3 \Pr m_6^2}{16\beta_1m_6^2 + 8 \Pr m_6 - \Pr \varphi},$$

$$B_{10} = \frac{-8A_2A_4 \Pr m_2m_6}{4\beta_1(m_2 + m_6)^2 + 4 \Pr(m_2 + m_6) - \Pr \varphi},$$

$$B_{11} = \frac{-4A_1^2 \Pr m_2^3}{16\beta_1m_2^2 + 8 \Pr m_2 - \Pr \varphi},$$

$$B_{12} = \frac{-4A_1A_2 \Pr m_6^2m_6}{4\beta_1(m_2 + m_6)^2 + 4 \Pr(m_2 + m_6) - \Pr \varphi},$$

$$B_{13} = \frac{-4A_1A_2 \Pr m_2^2m_6}{4\beta_1(m_2 + m_6)^2 + 4 \Pr(m_2 + m_6) - \Pr \varphi},$$

$$B_{14} = \frac{-4A_2^2 \Pr m_6^3}{16\beta_1m_6^2 + 8 \Pr m_6 - \Pr \varphi},$$

$$B_{15} = -(B_5 + B_6 + B_7 + B_8 + B_9 + B_{10} + B_{11} + B_{12} + B_{13} + B_{14}),$$

$$B_{16} = -\frac{2 \Pr A_1m_2C_1}{\beta_1(m_1 + m_2)^2 + \Pr(m_1 + m_2) - \frac{1}{4} \Pr(\phi - i\omega)},$$

$$B_{17} = -\frac{2 \Pr A_2m_6C_1}{\beta_1(m_1 + m_2)^2 + \Pr(m_1 + m_2) - \frac{1}{4} \Pr(\phi - i\omega)},$$

$$B_{18} = (1 - B_{16} + B_{17}),$$

$$B_{19} = \frac{2 \operatorname{Pr} A_1 m_2 C_2}{\beta_1 (m_1 + m_2)^2 + \operatorname{Pr} (m_1 + m_2) - \frac{1}{4} \operatorname{Pr} (\phi - i\omega)},$$

$$B_{20} = -\frac{2 \operatorname{Pr} A_2 m_6 C_2}{\beta_1 (m_1 + m_2)^2 + \operatorname{Pr} (m_1 + m_2) - \frac{1}{4} \operatorname{Pr} (\phi - i\omega)},$$

$$B_{21} = -\frac{2 \operatorname{Pr} A_1 m_2 C_3}{\beta_1 (m_1 + m_2)^2 + \operatorname{Pr} (m_1 + m_2) - \frac{1}{4} \operatorname{Pr} (\phi - i\omega)},$$

$$B_{22} = -\frac{2 \operatorname{Pr} A_2 m_6 C_3}{\beta_1 (m_1 + m_2)^2 + \operatorname{Pr} (m_1 + m_2) - \frac{1}{4} \operatorname{Pr} (\phi - i\omega)},$$

$$B_{23} = -\frac{2 \operatorname{Pr} A_3 C_1}{\beta_1 (m_1 + m_6)^2 + \operatorname{Pr} (m_1 + m_6) - \frac{1}{4} \operatorname{Pr} (\phi - i\omega)},$$

$$B_{24} = -\frac{2 \operatorname{Pr} A_4 C_1}{\beta_1 (m_1 + m_2)^2 + \operatorname{Pr} (m_1 + m_2) - \frac{1}{4} \operatorname{Pr} (\phi - i\omega)},$$

$$B_{25} = -\frac{2 \operatorname{Pr} A_5 C_1}{\beta_1 (m_1 + m_8)^2 + \operatorname{Pr} (m_1 + m_8) - \frac{1}{4} \operatorname{Pr} (\phi - i\omega)},$$

$$B_{26} = \frac{1}{4} \frac{i\omega m_1 m_6 A_2 C_1}{\beta_1 (m_1 + m_2)^2 + \operatorname{Pr} (m_1 + m_2) - \frac{1}{4} \operatorname{Pr} (\phi - i\omega)},$$

$$B_{27} = \frac{1}{4} \frac{i\omega m_1 m_6 A_2 C_1}{\beta_1 (m_1 + m_6)^2 + \operatorname{Pr} (m_1 + m_6) - \frac{1}{4} \operatorname{Pr} (\phi - i\omega)},$$

$$B_{28} = -\frac{m_1 m_2^2 A_1 C_1}{\beta_1 (m_1 + m_2)^2 + \operatorname{Pr} (m_1 + m_2) - \frac{1}{4} \operatorname{Pr} (\phi - i\omega)},$$

$$B_{29} = -\frac{m_1 m_6^2 A_2 C_1}{\beta_1 (m_1 + m_6)^2 + \operatorname{Pr} (m_1 + m_6) - \frac{1}{4} \operatorname{Pr} (\phi - i\omega)},$$

$$B_{30} = -\frac{m_2 m_1^2 A_1 C_1}{\beta_1 (m_1 + m_2)^2 + \operatorname{Pr} (m_1 + m_2) - \frac{1}{4} \operatorname{Pr} (\phi - i\omega)},$$

$$B_{31} = -\frac{m_6 m_1^2 A_2 C_1}{\beta_1 (m_1 + m_6)^2 + \operatorname{Pr} (m_1 + m_6) - \frac{1}{4} \operatorname{Pr} (\phi - i\omega)},$$

$$B_{32} = -(B_{19} + B_{20} + B_{21} + B_{22} + B_{23} + B_{24} + B_{25} + B_{26} + B_{27} + B_{28} \\ + B_{29} + B_{30} + B_{31}),$$

$$C_1 = \frac{G}{m_1^2 + m_1 - \left(M + \frac{i\omega}{4}\right)}, \quad C_2 = \frac{C_1 m_1^3}{m_1^2 + m_1 - \left(M + \frac{i\omega}{4}\right)},$$

$$C_3 = \frac{1}{4} \frac{i\omega C_1 m_1^2}{m_1^2 + m_1 - \left(M + \frac{i\omega}{4}\right)}.$$

REFERENCES

1. SOUNDALGEKAR V.M., POP I., Viscous dissipation effects on unsteady free convective flow past an infinite vertical porous plate with variable suction, *International Journal of Heat and Mass Transfer*, **17**(1): 85–92, 1974, doi: 10.1016/0017-9310(74)90041-6.
2. SINGH K.R., COWLING T.G., Thermal convection in magnetohydrodynamics: I. Boundary layer flow up a hot vertical plate, *The Quarterly Journal of Mechanics and Applied Mathematics*, **16**(1): 1–15, 1963, doi: 10.1093/qjmam/16.1.1.
3. SACHETI N.C., CHANDRAN P., SINGH A.K., An exact solution for unsteady magnetohydrodynamic free convective flow with constant heat flux, *International Communications in Heat and Mass Transfer*, **21**(1): 131–142, 1994, doi: 10.1016/0735-1933(94)90090-6.
4. SATTAR Md.A., ALAM Md.M., MHD free convective heat and mass transfer flow with Hall current and constant heat flux through a porous medium, *Indian Journal of Pure and Applied Mathematics*, **26**(2): 157–167, 1995.
5. SAHOO P.K., DATTA N., BISWAL S., Magnetohydrodynamic unsteady free convective flow past an infinite vertical plate with constant suction and heat sink, *Indian Journal of Pure and Applied Mathematics*, **34**(1): 145–155, 2003.
6. MAQBOOL K., MANN A.B., TIWANA M.H., Unsteady MHD convective flow of a Jeffery fluid embedded in a porous medium with ramped wall velocity and temperature, *Alexandria Engineering Journal*, **57**(2): 1071–1078, 2018, doi: 10.1016/j.aej.2017.02.012.
7. HAMZA M.M., Free convection slip flow of an exothermic fluid in a convectively heated vertical channel, *Ain Shams Engineering Journal*, **9**(4): 1313–1323, 2018, doi: 10.1016/j.asej.2016.08.011.
8. UN NISA Z., HAJIZADEH A., NAZAR M., Free convection flow of nanofluid over infinite vertical plate with damped thermal flux, *Chinese Journal of Physics*, **59**: 175–188, 2019, doi: 10.1016/j.cjph.2019.02.029.
9. HAJIZADEH A., SHAH N.A., SHAH S.I.S., ANIMASAUN I.L., GORJI M.-R., ALARIFI I.M., Free convection flow of nanofluids between two vertical plates with damped thermal flux, *Journal of Molecular Liquids*, **289**: Article ID 110964, 2019, doi: 10.1016/j.molliq.2019.110964.
10. SHAH N., ZAFAR A.A., FETEAU C., Free convection flows over a vertical plate that applies shear stress to a fractional viscous fluid, *Alexandria Engineering Journal*, **57**(4): 2529–2540, 2018, doi: 10.1016/j.aej.2017.08.023.
11. GHOLINIA M., HOSEINI M.E., GHOLINIA S., A numerical investigation of free convection MHD flow of Walters-B nanofluid over an inclined stretching sheet under the impact of Joule heating, *Thermal Science and Engineering Progress*, **11**: 272–282, 2019, doi: 10.1016/j.tsep.2019.04.006.

12. WANG Z.H., ZHOU Z.K., Eternal natural convection heat transfer of liquid metal under the influence of the magnetic field, *International Journal of Heat and Mass Transfer*, **134**: 175–184, 2019, doi: 10.1016/j.ijheatmasstransfer.2018.12.173.
13. PATEL H.R., Effects of cross diffusion and heat generation on mixed convective MHD flow of Casson fluid through porous medium with non-linear thermal radiation, *Heliyon*, **5**(4): 1–26, 2019, doi: 10.1016/j.heliyon.2019.e01555.
14. CHAMKHA A.J., Thermal radiation and buoyancy effects on hydromagnetic flow over an accelerating permeable surface with heat source or sink, *International Journal of Engineering Science*, **38**(15): 1699–1712, 2000, doi: 10.1016/S0020-7225(99)00134-2.
15. SATYA NARAYANA P.V., VENKATESWARLU B., VENKATARAMANA S., Thermal radiation and heat source effects on a MHD nanofluid past a vertical plate in a rotating system with porous medium, *Heat Transfer Asian Research*, **44**(1): 1–19, 2015, doi: 10.1002/htj.21101.
16. CORTELL R., MHD (magneto-hydrodynamic) flow and radiative nonlinear heat transfer of a viscoelastic fluid over a stretching sheet with heat generation/absorption, *Energy*, **74**: 896–905, 2014, doi: 10.1016/j.energy.2014.07.069.
17. AMIR HAMZAH N.S., KANDASAMY R., MUHAMMAD R., Thermal radiation energy on squeezed MHD flow of Cu, Al₂O₃ and CNTs-nanofluid over a sensor surface, *Alexandria Engineering Journal*, **55**(3): 2405–2421, 2016, doi: 10.1016/j.aej.2016.04.019.
18. FAGBADE A.I., FALODUN B.O., OMOWAYE A.J., MHD natural convection flow of viscoelastic fluid over an accelerating permeable surface with thermal radiation and heat source or sink: spectral homotopy analysis approach, *Ain Shams Engineering Journal*, **9**(4): 1029–1041, 2018, doi: 10.1016/j.asej.2016.04.021.
19. SATYA NARAYANA P.V., AKSHIT S.M., GHORI J.P., VENKATESWARLU B., Thermal radiation effects on an unsteady MHD nanofluid flow over a stretching sheet with non-uniform heat source/sink, *Journal of Nanofluids*, **6**(5): 899–907, 2017, doi: 10.1166/jon.2017.1374.
20. HARISH BABU D., AJMATH K.A., VENKATESWARLU B., SATYA NARAYANA P.V., Thermal radiation and heat source effects on MHD non-Newtonian nanofluid flow over a stretching sheet, *Journal of Nanofluids*, **8**(5): 1085–1092, 2018, doi: 10.1166/jon.2019.1666.
21. MAKANDA G., MAKINDE O.D., SIBANDA P., Natural convection of viscoelastic fluid from a cone embedded in a porous medium with viscous dissipation, *Mathematical Problems in Engineering*, **2013**: Article ID 934712, 11 pages, 2013, doi: 10.1155/2013/934712.
22. VENKATESWARLU B., SATYA NARAYANA P.V., Influence of variable thermal conductivity on MHD Casson fluid flow over a stretching sheet with viscous dissipation, Soret and Dufour effects, *Frontiers in Heat and Mass Transfer*, **7**(1): 1–9, 2016, doi: 10.5098/hmt.7.16.
23. HAYAT T., IJAZ KHAN M., WAQAS M., YASMEEN T., ALSAEDI A., Viscous dissipation effect in flow of magnetonanofluid with variable properties, *Journal of Molecular Liquids*, **222**: 47–54, 2016, doi: 10.1016/j.molliq.2016.06.096.
24. NAYAK M.K., MHD 3D flow and heat transfer analysis of nanofluid by shrinking surface inspired by thermal radiation and viscous dissipation, *International Journal of Mechanical Sciences*, **124–125**: 185–193, 2017, doi: 10.1016/j.ijmecsci.2017.03.014.
25. KHAN M.I., HAYAT T., KHAN M.I., ALSAEDI A., A modified homogeneous-heterogeneous reactions for MHD stagnation flow with viscous dissipation and Joule heating, *International Journal of Heat and Mass Transfer*, **113**: 310–317, 2017, doi: 10.1016/j.ijheatmasstransfer.2017.05.082.

26. HAYAT T., KHAN M.I., ALSAEDI A., KHAN M.I., Joule heating and viscous dissipation in flow of nanomaterial by a rotating disk, *International Communications in Heat and Mass Transfer*, **89**: 190–197, 2017, doi: 10.1016/j.icheatmasstransfer.2017.10.017.
27. RAMESH K., Effects of viscous dissipation and Joule heating on the Couette and Poiseuille flows of a Jeffery fluid with slip boundary conditions, *Propulsion and Power Research*, **7**(4): 329–341, 2018, doi: 10.1016/j.jprr.2018.11.008.
28. MUHAMMAD T., HAYAT T., SHEHZAD S.A., ALSAEDI A., Viscous dissipation and Joule heating effects in MHD 3D flow with heat and mass fluxes, *Results in Physics*, **8**: 365–371, 2018, doi: 10.1016/j.rinp.2017.12.047.
29. VENKATESWARLU B., SATYA NARAYANA P.V., TARAKARAMU N., Melting and viscous dissipation effects on MHD flow over a moving surface with constant heat source, *Transactions of A. Razmadze Mathematical Institute*, **172**(3B): 619–630, 2018, doi: 10.1016/j.trmi.2018.03.007.
30. EZZAT M.A., ABD-ELAAL M.Z., Free convection effects on a viscoelastic boundary layer flow with one relaxation time through a porous medium, *Journal of the Franklin Institute*, **334**(4): 685–706, 1997, doi: 10.1016/S0016-0032(96)00095-6.
31. PRASAD K.V., PAL D., UMESH V., PRASANNA RAO N.S., The effect of variable viscosity on MHD viscoelastic fluid flow and heat transfer over a stretching sheet, *Communication in Non-Linear Science and Numerical Simulation*, **15**(2): 331–344, 2010, doi: 10.1016/j.cnsns.2009.04.003.
32. GOYAL M., BHARGAVA R., Numerical solution of MHD viscoelastic nanofluid flow over a stretching sheet with partial slip and heat source/sink, *ISRN Nanotechnology*, **2013**: Article ID 931021, 11 pages, 2013, doi: 10.1155/2013/931021.
33. RASHIDI M.M., ALI M., FREIDONIMEHR N., ROSTAMI B., HOSSAIN M.A., Mixed convective heat transfer for MHD viscoelastic fluid flow over a porous wedge with thermal radiation, *Advances in Mechanical Engineering*, **6**, 2014, doi:10.1155/2014/735939.
34. VENKATESWARLU B., SATYA NARAYANA P.V., MHD visco-elastic fluid flow over a continuously moving vertical surface with chemical reaction, *Walailak Journal of Science and Technology*, **12**(9): 775–783, 2015.
35. LI J., ZHENG L., LIU L., MHD viscoelastic flow and heat transfer over a vertical stretching sheet with Cattaneo-Christov heat flux effects, *Journal of Molecular Liquids*, **221**: 19–25, 2016, doi: 10.1016/j.molliq.2016.05.051.
36. BILAL S., MALIK M.Y., AWAIS M., KHALIL-UR-REHMAN, HUSSAIN A., KHAN I., Numerical investigation on 2D viscoelastic fluid due to exponentially stretching surface with magnetic effects: an application of non-Fourier flux theory, *Natural Computing and Applications*, **30**(9): 2749–2758, 2018, doi: 10.1007/s00521-016-2832-4.
37. SATYA NARAYANA P.V., TARAKARAMU N., MAKINDE O.D., VENKATESWARLU B., SAROJAMMA G., MHD stagnation point flow of viscoelastic nanofluid past a convectively heated stretching surface, *Defect and Diffusion Forum*, **387**: 106–120, 2018, doi: 10.4028/www.scientific.net/DDF.387.106.
38. CHOUDHURY R., DEY D., Free convective MHD flow of a non-Newtonian fluid past an infinite vertical plate with constant suction and heat sink, *International Journal of Dynamics of Fluids*, **8**(2): 83–94, 2012.

39. DESSIE H., KISHAN N., MHD effects on heat transfer over stretching sheet embedded in porous medium with variable viscosity, viscous dissipation and heat source/sink, *Engineering Physics and Mathematics. Ain Shams Engineering Journal*, **5**(3): 967–977, 2014, doi: 10.1016/j.asej.2014.03.008.
40. BESTHAPU P., UL HAQ R., BANDARI S., AL-MDALLAL Q.M., Mixed convection flow of thermally stratified MHD nanofluid over an exponentially stretching surface with viscous dissipation effect, *Journal of the Taiwan Institute of Chemical Engineers*, **71**: 307–314, 2017, doi: 10.1016/j.jtice.2016.12.034.

Received May 19, 2021; accepted version November 9, 2021.

Published on Creative Common licence CC BY-SA 4.0

